Investigation of the nonlinear CPT spectrum of ^{87}Rb and its application for large dynamic magnetic measurement*

Chi Xu(徐迟)[1,2], Shi-Guang Wang(王时光)[2,3], Yong Hu(胡勇)[2,3], Yan-Ying Feng(冯焱颖)[2,3,†] and Li-Jun Wang(王力军)[1,2,3,‡]

[1] *Department of Physics, Tsinghua University, Beijing* 100084, *China*
[2] *Joint Institute for Measurement Science, Tsinghua University, Beijing* 100084, *China*
[3] *State Key Laboratory of Precision Measurement Technology and Instrument, Tsinghua University, Beijing* 100084, *China*

(Received 27 December 2016; revised manuscript received 13 February 2017; published online 20 April 2017)

The coherent population trapping (CPT) phenomenon has found widespread application in quantum precision measurements. Various designs based on the narrow resonant spectrum corresponding to the linear Zeeman effect have been demonstrated to achieve high performance. In this article, the nonlinear Zeeman split of the CPT spectrum of ^{87}Rb in the lin||lin setup is investigated. We observe re-split phenomenon for both magnetic sensitive and magnetic insensitive CPT resonant lines at a large magnetic field. The re-split in the magnetic sensitive lines raises a practical problem to magnetometers worked in the lin||lin setup while the other one shows a good potential for applications in large magnetic field. We propose a design based on the nonlinear split of the magnetic insensitive lines and test its performance. It provides a much larger measurement range compared to the linear one, offering an option for atomic magnetometers where a large dynamic range is preferred.

Keywords: coherent population trapping, nonlinear Zeeman effect, large dynamic magnetometer

PACS: 42.50.Gy, 32.60.+i, 07.55.Ge **DOI:** 10.1088/1674-1056/26/6/064203

1. Introduction

In recent years, magnetometers based on the CPT resonant spectrum have found their applications in various fields like navigation,[1,2] geomagnetic mapping,[3,4] bioscience,[5–8] and fundamental physics.[9] These magnetometers are all in the optical setup and are convenient for miniaturization. High sensitivity of the pT/$\sqrt{\text{Hz}}$ level has been achieved by many designs.[7,10–14] These magnetometers measure the external magnetic field by monitoring the frequency shifts of the different Zeeman resonance transmission peaks of the CPT spectrum. To gain a high SNR (signal-to-noise ratio), methods like lin||lin setup or push-pull pumping have been introduced in these magnetometers to overcome the unwanted population pumped by the circularly polarized light.[15,16] The spectrum of the lin||lin setup, however, is more complex compared to the circularly polarized one due to the various possible combinations for CPT among the energy levels. For magnetometers worked in lin||lin setup, the frequency difference between the Zeeman levels with different magnetic quantum number m_{F} behaves quite linearly with low external magnetic field. While for a relatively large magnetic field, the Zeeman levels will split nonlinearly: the original transition peak re-splits at a certain magnetic field, which will cause problems for magnetometers loop-locked to the peak and limit the dynamic range. In this article we first investigate the nonlinear Zeeman CPT spectrum of ^{87}Rb in a buffer gas cell with the lin||lin setup and show its good potential for large magnetic field measurements. We then propose a double FM (frequency modulation) modulation measurement design based on the nonlinear Zeeman effect and test its performance. It provides several advantages. First, this measurement performs an absolute magnetic field measurement. In addition, this measurement has a much larger dynamic range than the one based on the linear Zeeman effect and remains a linear response. Finally, the double FM modulation technique enables the magnetometer to monitor the magnetic field by the measurement of the frequency signal instead of the amplitude signal.[10] This proposal offers an option for atomic magnetometers for large magnetic field applications.

2. Nonlinear CPT spectrum and applications for magnetic measurement

A typical CPT system can be simplified as a three levels Λ structure. For practical applications of magnetometers based on alkali metal atoms, the two lower levels usually come from the ground hyperfine states with different magnetic quantum number m_F. In the presence of the external magnetic field, these energy levels will shift according to the Breit–Rabi

*Project supported by the National Natural Science Foundation of China (Grant No. 61473166) and China Postdoctoral Science Foundation (Grant No. 014M560958).

†Corresponding author. E-mail: yyfeng@tsinghua.edu.cn
‡Corresponding author. E-mail: lwan@tsinghua.edu.cn

© 2017 Chinese Physical Society and IOP Publishing Ltd

formula.[17] If the magnetic field is small enough that the linear approximation is valid, the energy difference among the hyperfine levels will be proportional to the field B. By tracking the magnetic sensitive resonant peak in the CPT spectrum, one can obtain the information of the external field. While at a relatively larger field, the nonlinear effect cannot be neglected. Thus the CPT spectrum will be more complicated according to the specific pumping process. In the lin||lin pumping setup, the nonlinear effect will lead to a re-split of the original CPT peaks which introduces some practical problems. First, the relationship between the output of the magnetometer and magnetic field can no longer be linear where corrections have to be taken to compensate the nonlinear term. Second, for loop-locked magnetometers, there exist problems at the moment when re-split happens since nothing can guarantee which peak the magnetometer is still locked to after the re-split. This will limit the dynamic range of this kind of magnetometer in high sensitivity magnetic field measurement.

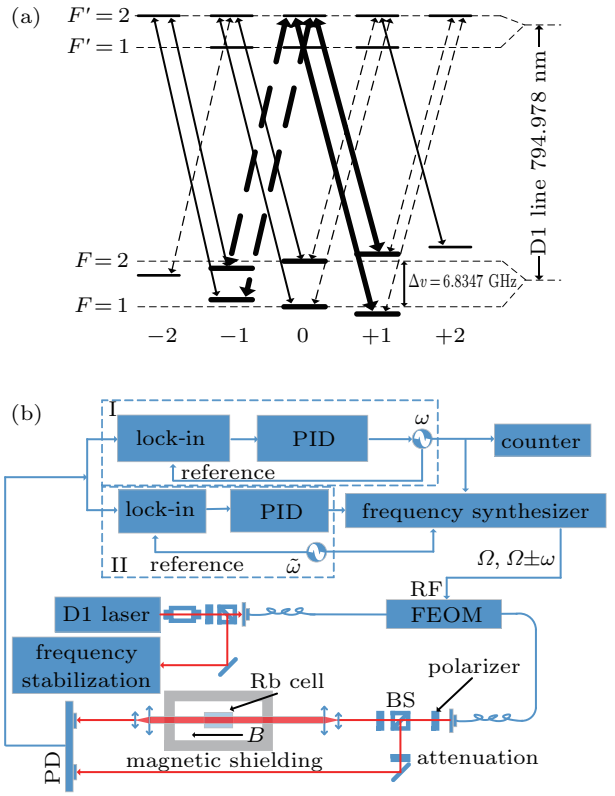


Fig. 1. (color online) (a) Energy level of the ^{87}Rb atom with the $F = 2 \to F'$ transition. The σ^+ and σ^- component of the linear polarized light are plotted as dash and solid lines, respectively. The levels belonging to the group $N = 0$ are plotted with bold lines. These resonances result in 7 resonant peaks in the CPT spectrum which can be classified to 3 groups due to their behavior in the external field. For simplicity, the energy shift of the excited levels is not shown. (b) Schematic diagram of the electric and optical layout of the system. Control sections 1 and 2 are shown in the dash boxes. The quarter-wave plate is for observation of the CPT spectrum excited by differently polarized light. In the lin||lin configure for the magnetometer experiment, the fast axis of the quarter-wave plate is set along the polarization of the linearly polarized light.

We illustrate the nonlinear Zeeman split with ^{87}Rb atom (Fig. 1(a)) pumped by the D1 line. The hyperfine structure of ^{87}Rb atom can form 7 combinations in the lin||lin pumping setup which result in 7 resonant peaks in the CPT spectrum. According to the relationship with the external field in the linear approximation $\Delta E = N\hbar\gamma B = Ng_{\rm F}\mu_{\rm B}B$, where $g_{\rm F}$ is the absolute value of the landé "g-factor", $\hbar$ is the Planck constant and γ is the gyromagnetic ratio, these resonant peaks can be classified into three groups with $N = \pm 2, 0$. The group with $N = 0$ includes three components: $(|F = 2, m_F = -1\rangle, |F = 1, m_F = +1\rangle)$, $(|F = 2, m_F = 0\rangle, |F = 1, m_F = 0\rangle)$ and $(|F = 2, m_F = +1\rangle, |F = 1, m_F = -1\rangle)$. While at a large field, each group will re-split due to the nonlinear terms in the Breit–Rabi formula,

$$E_{|J=\frac{1}{2},m_{\rm J},I,m_{\rm I}\rangle} = -\frac{\Delta E_{\rm hfs}}{2(2I+1)} + g_{\rm I}\mu_{\rm B}mB \pm \frac{\Delta E_{\rm hfs}}{2}\left(1 + \frac{4mx}{2I+1} + x^2\right)^{1/2} \quad (1)$$

$$x = \frac{(g_{\rm J} - g_{\rm I})\mu_{\rm B}B}{\Delta E_{\rm hfs}}, \quad (2)$$

where the $\Delta E_{\rm hfs}$ is the hyperfine splitting of ^{87}Rb, $g_{\rm I}$ is the nuclear g-factor, $g_{\rm J}$ is the fine structure landé "g-factor" of $5^2S_{1/2}$, $m = m_{\rm I} \pm m_{\rm J}$ (the $\pm$ sign is the same with the one in the formula). The specific value of these coefficients for calculation and more detailed information of Breit–Rabi formula can be found in Reference.[18] Thus one can figure out that for a lin||lin setup magnetometer monitoring the $N = +2$ resonant peak with a linewidth narrower than 1 kHz, re-split will happen at a field below 350 mGs (1 Gs = 10^{-4} T), which is even smaller than the Earth's field. Since a much narrower resonant peaks is preferable in the high precision measurement, the re-split will greatly limit the dynamic range of these magnetometers.

The peaks with $N = 0$ will re-split as well. We observe the re-split for both $N = +2$ (Fig. 2(a) insert) and $N = 0$ (Fig. 2(b)). It is noted that from the formula Eq. (1), the frequency difference between the two peaks (indicated by the bold Λ structures in Fig. 1(a)) within the $N = 0$ group remains linear:

$$\Delta E = 4g_{\rm I}\mu_{\rm B}B = \hbar\tilde{\gamma}B. \quad (3)$$

The formula refers the frequency shift to the external field B directly through the nuclear landé "g-factor" which also offers a way to measure $g_{\rm I}$ directly. The frequency difference of the two peaks can be used to monitor the external field B. The advantage and disadvantage are both obvious: First, the relationship between the frequency shift and the external field remains linear as long as the Breit–Rabi formula is valid; second, the measurement is absolute due to the measurement of the frequency difference between the two CPT peaks; finally, because of the smaller effective gyromagnetic ratio $g_{\rm I}$ (which is much smaller than $g_{\rm J}$[19]), the magnetometer provides a large

dynamic range with a relatively reduced sensitivity. In applications such as the unshielded large field measurements, the ambient magnetic noise can be larger than the intrinsic noise of the high sensitivity magnetometer itself, making it suitable to sacrifice the sensitivity to gain other properties like the large field measurement.

We propose a magnetometer design based on the re-split of the CPT spectrum at large field as an extra operation option for the linear effect. To realize the measurement of the frequency difference between the two individual resonance peaks simultaneously, we introduce the double-FM technology to form a closed-loop operation. The coherent pumping light for CPT is obtained from a FEOM (fiber electro-optic modulator) with its RF signal controlled by a local oscillator at the frequency of the hyperfine split of ^{87}Rb. We add another frequency modulation to the driving RF signal, creating new sidebands beside the carrier. Local maximum will occur if the carrier and the sideband resonant with the two CPT transition simultaneously. Thus by tracking the frequency of the added modulation we can determine the frequency difference between the two CPT peaks.

3. Experimental setup and results

The schematic diagram of the optical and electronic components in our experiment is shown in Fig. 1(b). An isotopically pure ^{87}Rb cylindrical cell serves as the atom source, with approximately 10 Torr (1 Torr = 1.33322×10^2 Pa) of Ne as the buffer gas. The cell is 20 mm in diameter and 60 mm in length. The pumping light (795 nm with linewidth below 1 MHz) comes from an external cavity diode laser (DL 100, Toptica) resonant with the D1 transition line of ^{87}Rb. Part of the light is split to stabilize the laser's frequency using the AC Zeeman frequency stabilization. The remaining light passes through the FEOM through fiber to generate the coherent component for CPT pumping. The FEOM is driven by an RF signal from a frequency synthesizer. The synthesizer gives the RF signal at the frequency of 6.834 GHz which meets the hyperfine split of ^{87}Rb. The sidebands needed to simultaneously excite the two CPT resonances is produced by feeding an extra signal at a frequency ω to the FM port of the synthesizer. Thus, the spectrum of the output driven RF signal will have frequency components at Ω, $\Omega\pm\omega$. The power of the RF is optimized to make the CPT signal maximum. After the FEOM, the light passes a polarizer, and a quarter-wave plate in sequence, then pumps and probes the alkali atoms in the cell. The cell is held in a self-wrapped magnetic shielding tube with μ-metal tape. The inside solenoid generates the homogeneous magnetic field $\boldsymbol{B}$ over the cell. The laser beam is expanded to 10 mm in diameter before entering the cell and is focused for detection. We use a differential balanced detection setup to reduce the influence of the intensity fluctuation of the laser light and remove the bias. In the closed-loop operation, the signal of the PD is fed back to the control sections. A third sinusoidal modulation, whose frequency $\widetilde{\omega}$ is tuned far away from ω to avoid crosstalk, is used in the control section 2 to help locking one of the two CPT peaks ($(|F=2,m_F=+1\rangle,|F=1,m_F=-1\rangle)$ or $(|F=2,m_F=-1\rangle,|F=1,m_F=+1\rangle)$) while the control section 1 locks ω which can be directly read out from the frequency counter and monitor the external field. The cell is at room temperature during all experiments.

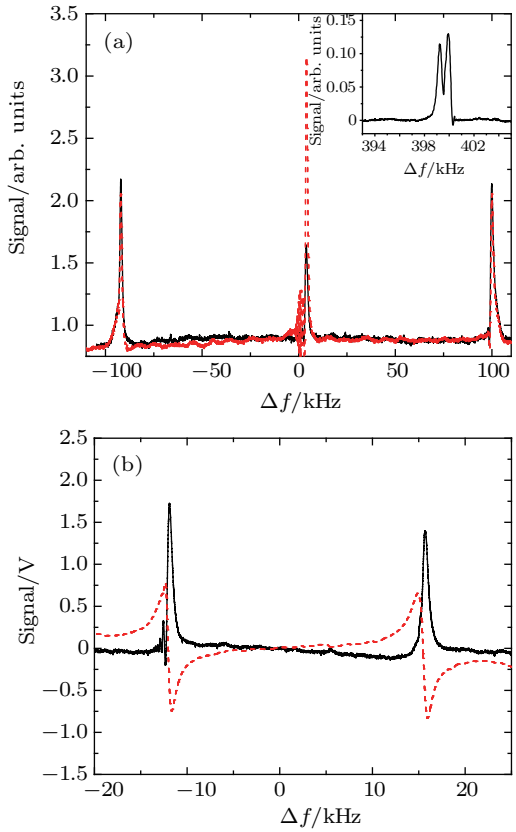


Fig. 2. (color online) (a) Linear CPT spectrum observed in the lin||lin configure. The FWHM (full width at half maximum) of the peak at 100 kHz is about 1 kHz (dash line: $F=2\rightarrow F'=1$, solid line: $F=2\rightarrow F'=2$). Insert: nonlinear split of the $N=+2$ at a magnetic field about 280 mGs. This spectrum is observed at a relatively low light intensity with an FWHM of 600 Hz. (b) Nonlinear split of the magnetic insensitive CPT resonant peaks. Observation of the two re-split resonant peaks (solid line) in group $N=0$ at a large magnetic field, together with their error signal (dash line) after the lock-in amplifier in the control section 2. The resonant peak at the middle is almost covered by noise due to destructive interference.

Figure 2(a) shows a usual linear CPT spectrum with resonant peaks $N=0,\pm2$ at a small external field. The linewidth is about 1 kHz, mainly due to the light broadening. We measure the CPT spectrum for $F=2\rightarrow F'=1$ and $F=2\rightarrow F'=2$ transitions, respectively. The relative amplitude between the $N=0$ peak and the $N=+2$ one is quite different, which offers options for particular application of the magnetometers or atomic clocks.[20] We also show the re-split of the $N=+2$ happening at a magnetic field of 280 mGs. The frequency difference between the re-split peaks is about 700 Hz, which

will contribute an error of about 0.2% if the magnetometer is locked to the wrong peak after the re-split. Such an error cannot be neglected in precision measurement especially when the field is comparable to or larger than the geomagnetic field. For a high sensitivity CPT magnetometer with a linewidth much narrower, the magnetic field for the re-split occurrence will become much smaller, significantly limiting the dynamic range.

The nonlinear CPT splitting of the $N = 0$ group with the lin||lin setup is observed and shown in Fig. 2(b) with the $F = 2 \rightarrow F' = 1$ transition at a magnetic field of 5 Gs. Due to a destructive interference effect, the CPT constructed by the states $|F = 1, m_F = 0\rangle$ and $|F = 2, m_F = 0\rangle$ is at minimum.[21] To verify the linear relation of Eq. (3), we measure the resonant frequency of the two peaks respectively in the open loop operation. The magnetic field range is tested up to 30 Gs limited by our current source. The magnetic field generated by the solenoid with respect to its current is measured by a fluxgate first. The result is shown in Fig. 3(a), which shows a good agreement. The slope is estimated to be (5.58 ± 0.02) kHz/Gs in a good agreement with the calculation of 5.57 kHz/Gs using Eq. (3). The primary uncertainty comes from the measurement of the solenoid current.

We then test the closed-loop operation. The magnitude of the magnetic field to be measured is around 5 Gs which is far larger than the geomagnetic field. With the help of the error signal from the lock-in amplifier in loop II we can lock the carrier frequency Ω at one of the two CPT peaks in group $N = 0$. Then, we turn on the frequency modulation of the synthesizer which generates the sidebands at $\Omega \pm \omega$. When ω scans over the resonant point of the other CPT peak in group $N = 0$, the quadrature component of the lock-in amplifier gives a dispersive line shape. At the zero point of the lock-in amplifier output, ω is locked to the frequency difference of the two CPT peaks which reveals the external magnetic field. We test the noise performance by recording ω in the closed-loop operation for 20 s with a sampling rate at 500 Hz. We analyze the FFT spectrum of the recording signal which shows a sensitivity about 2.4 nT/$\sqrt{\text{Hz}}$ in average from 1 Hz to 100 Hz. The electric noise of the control sections is found to be negligible and the sensitivity is mainly limited by the noise of the laser light and the weak resonant signal. Since the cell is set under room temperature, improvement on sensitivity can be achieved by heating. We repeat the experiment at the same condition except that the self-wrapped magnetic shielding is removed to investigate the performance when the cell is exposed to the geomagnetic environment and other magnetic noises in the lab. Since the effective gyromagnetic ratio of the nonlinear Zeeman is much smaller compared to the linear one, measurements based on the nonlinear splitting will be less sensitive to the magnetic gradient, to which high sensitive magnetometers are usually susceptible. We observe a 2.5 times worsening in performance, with a noise level of 6 nT/$\sqrt{\text{Hz}}$ on average from 1 Hz to 100 Hz. The results are shown in Fig. 3(b).

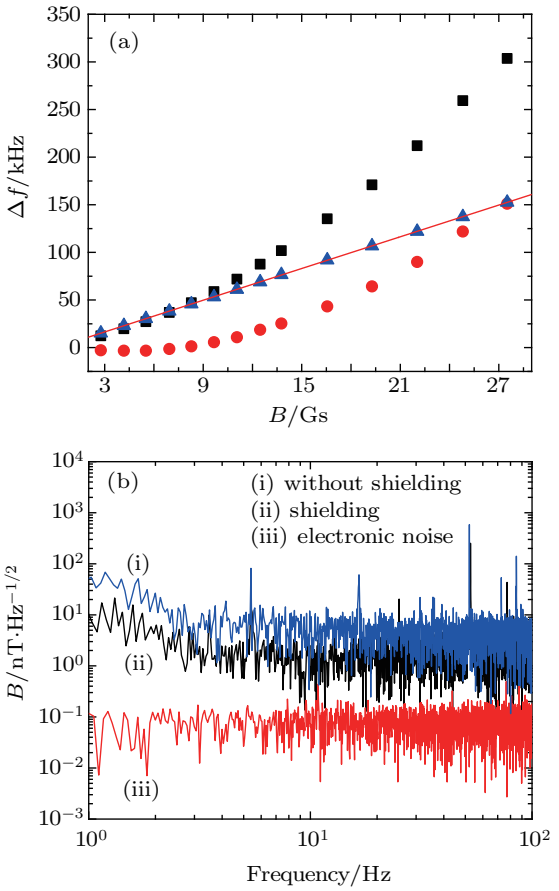


Fig. 3. (color online) (a) Checking of the linear relationship given by Eq. (3). The squares and dots represent the frequency shift vs external magnetic field B of the two peaks in group $N = 0$, respectively and the triangles represent the frequency difference between the two peaks. The red line is the linear fit which shows a good agreement with Eq. (3). (b) Effective magnetic noise density spectrum. The data above shows the noise performance of the measurement based on the nonlinear split of group $N = 0$ in the double modulation loop-lock operation (ii), compared with an operation in the same condition but without magnetic shielding (i). The plot (iii) shows the electric noise of the system. The data is all normalized to 1Hz bin.

4. Conclusion

In summary, we investigate the nonlinear splitting of the CPT spectrum in a lin||lin setup of ^{87}Rb and observe the re-split of the CPT spectrum. Based on the nonlinear Zeeman effect we propose and demonstrate a larger dynamic range, absolute magnetometer with a sensitivity about 2.4 nT/$\sqrt{\text{Hz}}$ at room temperature. Further work will include optimizing the cell temperature and reducing the noise of the laser light to improve the sensitivity. The double frequency modulation method which locks the two peaks simultaneously can also be applied to the linear Zeeman split. Thus the magnetometers utilizing this technique can switch freely between the linear and nonlinear operation setups depending on particular applications where high sensitivity or large dynamic range is preferred.

Acknowledgment

The authors thank Shuo Jiang for the isotopically pure ^{87}Rb cells.

References

[1] Alipieva E, Andreeva C, Avramov L, Bevilaqua G, Biancala V, Borisova E, Breschi E, Cartaleva S, Dancheva Y, Gateva S, Karaulanov T, Lammegger R, Moi L, Petrov L, Petrov N, Slavov D, Taskova E, Todorov G, Windholz L and Yanev A 2005 *Proceedings of the Society of Photo-Optical Instrumentation Engineers* (SPIE) 13th International School on Quantum Electronics, September 20–24, 2004, Bourgas, Bulgaria, pp. 170–175

[2] Reigber C, Luhr H and Schwintzer P 2002 *Advances in Space Research* (Adv. Space Res.) Symposium of COSPAR Scientific Commission B held at the 33rd COSPAR Scientific Assembly, July, 2000, Warsaw, Poland, pp. 129–134

[3] Sheng D, Li S, Dural N and Romalis M V 2013 *Phys. Rev. Lett.* **110** 160802

[4] Nabighian M N, Ander M E, Grauch V J S, Hansen R O, LaFehr T R, Li Y, Pearson W C, Peirce J W, Phillips J D and Ruder M E 2005 *Geophysics* **70** 63ND

[5] Stahler M, Wynands R, Knappe S, Kitching J, Hollberg L, Taichenachev A and Yudin V 2002 *Opt. Lett.* **27** 1472

[6] Kominis I K, Kornack T W, Allred J C and Romalis M V 2003 *Nature* **422** 596

[7] Kitching J, Knappe S, Shah V, Schwindt P, Griffith C, Jimenez R, Preusser J, Liew L A and Moreland J 2008 *IEEE International Frequency Control Symposium*, May 19–21, 2008, Honolulu, HI, USA, pp. 789–794

[8] Knappe S, Schwindt P, Gerginov V, Shah V, Brannon A, Lindseth B, Liew L A, Robinson H, Moreland J, Popovic Z, Hollberg Leo and Kitching J 2007 *Proceedings of the Socity of Photo-OPtical Instrumentation Engineers* (SPIE) 14th International School on Quantum Electronics on Laser Physics and Applications, Septemper 18–22, 2006, Sunny Beach, Bulgaria, p. 60403

[9] Vasilakis, G, Brown J M, Kornack T W and Romalis M V 2009 *Phys. Rev. Lett.* **103** 261801

[10] Hu Y, Feng Y Y, Xu C, Xue H B and Sun L 2014 *Appl. Opt.* **53** 2158

[11] Lenci L, Auyuanet A, Barreiro S, Valente P, Lezama A and Failache H 2014 *Phys. Rev. A* **89** 043836

[12] Schwindt P, Knappe S, Shah V, Hollberg L, Kitching J and Liew L and Moreland J 2004 *Appl. Phys. Lett.* **85** 6409

[13] Liu G B, Sun X P, Gu S H, Feng J W and Zhou X 2012 *Physics* **41** 803 (in Chinese)

[14] Zhang F, Tian Y, Zhang Y and Gu S H 2016 *Chin. Phys. B* **25** 094206

[15] Jau Y, Miron E, Post A, Kuzma, N and Happer W 2004 *Phys. Rev. Lett.* **93** 160802

[16] Taichenachev A, Yudin V, Velichansky V and Zibrov S 2005 *JETP Lett.* **82** 398

[17] Breit G and Rabi I 1931 *Phys. Rev.* **38** 2082

[18] Steck D A http://steck.us/alkalidata/ (2010)

[19] Arimondo E, Inguscio M and Violino P 1977 *Rev. Mod. Phys.* **49** 31

[20] Sun X L, Zhang J W, Cheng P F, Xu C, Zhao L and Wang L J 2016 *Opt. Express* **24** 4532

[21] Levi F, Godone A, Vanier J, Micalizio S and Modugno G 2000 *Eur. Phys. J. D* **12** 53